

THE BOLTZMANN EQUATION AS CELLULAR AUTOMATON: A NEW SIMULATION TECHNIQUE

K. Kometer, G. Zandler, P. Vogl, and E. Gornik

Physik Department and Walter Schottky Institut, TU Munchen, D-8046 Garching, FRG

Abstract

We show that the semiclassical Boltzmann equation for nonlinear transport in semiconductors can be converted into a cellular automaton with only nearest neighbor interactions in position space. This procedure leads to a new and numerically highly efficient simulation technique for inhomogeneous high field transport. Excellent agreement with Monte Carlo results for homogeneous as well as inhomogeneous and transient transport in GaAs is obtained.

A. Introduction

Recently, a new simulation strategy has been developed in fluid dynamics [1,2]. The standard kinetic approach starts from the discrete, atomistic point of view with many degrees of freedom. By making use of conservation laws and sophisticated gradient expansions, one eliminates most of these variables and obtains the continuous Navier–Stokes equations which depend only on a few macro-variables. Since these equations cannot be solved analytically, however, the conventional procedure is to replace them again by a discrete “microworld” with many degrees of freedom and dynamical laws that follow from the discretization process. This discrete microdynamics is often numerically unstable (e.g., in turbulent flow). Facing this whole procedure, Hardy et al. [3] and Frisch et al. [1,2] raised the question whether it is possible to find a *fictional microworld* obeying a simple and numerically stable dynamics that yields the *same macroscopic dynamics* as the real physical system. Indeed, they were able to show that an exceedingly simple microdynamics can be found that obeys the Navier-Stokes equations in the macroscopic limit. This microdynamics constitutes a cellular automaton. A cellular automaton consists of a lattice, each site of which has a finite number of states [4]. Cellular automata (CA) evolve in discrete time steps, all sites being simultaneously updated. The dynamics of CA are governed by local rules, i.e. the updating of site variables involves only a small number of neighbors in each time step. For this reason, CA constitute one of the very few algorithms for physical processes which can optimally utilize massively parallel computer technology. In addition, the locality of the dynamical rules allows an efficient and flexible treatment of complex topologies and is numerically stable by construction since only Boolean variables are involved [4].

The major characteristics of CA are the two length scales they operate on. First, there is the discrete microworld on a lattice obeying a *fictional dynamics* of pseudo-particles. The length and time scales for this dynamics are much shorter than the physical scales. Second, there is the continuous macroscale with the physical observables, which are obtained in practice by taking averages over many cells.

In this paper, we extend these ideas to a nonlocal integro-differential equation which contains intrinsically many degrees of freedom, namely the Boltzmann equation (BE) for charged carrier transport in semiconductors. We show that the full nonlocal BE can be successfully transformed into a Boolean master equation or cellular automaton which contains only *local* interactions in position space [5]. On the microscale of this CA, this transformation effectively decouples the spatial and momentum variables. This

grossly simplifies the solution of the BE particularly for strongly inhomogeneous situations and complex device geometries. We obtain a new, robust technique for transport simulations which is comparable in accuracy to the Monte Carlo method [6,7], automatically tailored to modern parallel and vector processors, and accessible to analytical solutions in limiting cases. We show that the CA rules can be systematically calculated, based on the quantum mechanical scattering rates and the equations of motion for the electrons.

The cellular automaton that follows from the semiclassical BE has the following properties. It is defined on a lattice in real space (\mathbf{x} space) and attached to each lattice site, there is a complete set of \mathbf{k} states which we term \mathbf{k} cells. These sites \mathbf{x} and \mathbf{k} cells are populated by fictitious particles obeying non-deterministic dynamical rules. These rules consist of (i) on-site transitions between the discrete \mathbf{k} cells representing scattering events in \mathbf{k} space, and (ii) translations between equivalent \mathbf{k} cells on neighboring lattice sites \mathbf{x} giving the carriers' real space motion on the macroscale of the CA.

B. Theory

The BE for the single particle distribution function $f = f(\mathbf{x}, \mathbf{k}; t)$ reads

$$\frac{\partial f}{\partial t} = - \left. \frac{\partial f}{\partial t} \right|_E + \left. \frac{\partial f}{\partial t} \right|_{coll} . \quad (1)$$

The collision term contains the total quantum mechanical scattering probability per unit time due to elastic and inelastic processes. For nondegenerate electrons, it has the form

$$\left. \frac{\partial f}{\partial t} \right|_{coll} = \frac{V}{(2\pi)^3} \int d\mathbf{k}' \{ w(\mathbf{x}, \mathbf{k}', \mathbf{k}) f(\mathbf{x}, \mathbf{k}'; t) - w(\mathbf{x}, \mathbf{k}, \mathbf{k}') f(\mathbf{x}, \mathbf{k}; t) \} . \quad (2)$$

In these equations, V is the crystal volume and $w(\mathbf{x}, \mathbf{k}', \mathbf{k})$ the scattering probability per unit time from Bloch state \mathbf{k}' into state \mathbf{k} . In the form of Eq. (2), the collision term is sufficiently general to allow the inclusion of all types of elastic and inelastic one-particle scattering mechanisms such as phonons, impurities, disorder, and boundaries [7]. We point out that the collision term Eq. (2) is local in position space. This locality is a basic assumption underlying the Boltzmann equation.

If the BE contained only the collision term on the right hand of Eq. (1), the resulting equations would constitute simple rate (master) equations that depend only parametrically on the position \mathbf{x} . In contrast, the kinematic terms in the BE,

$$\left. \frac{\partial f}{\partial t} \right|_E = \dot{\mathbf{x}} \nabla_{\mathbf{x}} f(\mathbf{x}, \mathbf{k}; t) + \dot{\mathbf{k}} \nabla_{\mathbf{k}} f(\mathbf{x}, \mathbf{k}; t) , \quad (3)$$

supplemented by the equations of motion for Bloch wave packets of momentum \mathbf{k} , charge $-e$, and energy dispersion $\varepsilon(\mathbf{k})$,

$$\begin{aligned} \dot{\mathbf{x}} &= \frac{1}{\hbar} \nabla_{\mathbf{k}} \varepsilon(\mathbf{k}) , \\ \dot{\mathbf{k}} &= -\frac{e}{\hbar} \mathbf{E}(\mathbf{x}) , \end{aligned} \quad (4)$$

are highly nonlocal functions both in position and momentum space which link the distribution function $f(\mathbf{x}, \mathbf{k}; t)$ to its value in different $(\mathbf{x}', \mathbf{k}')$ -locations. Consequently, the major obstacle in converting the BE to a *local* CA is not the collision term but the explicit nonlocality of the kinematic terms.

In the standard ensemble Monte Carlo method, the solution of the BE is achieved by solving in turns the rate equations Eq. (2) and the microscopic equations of motion Eq. (4) for each particle [6,7]. This

requires a frequent switching between two representations of the particle ensemble, namely a collective probabilistic description and a deterministic description of individual particle trajectories which conserve energy and momentum precisely. We will show here that it is possible to solve the BE entirely within a collective probabilistic description.

The main result of this work is that the kinematic terms Eq. (3) in the BE can be transformed into effective collision terms that have the same form as Eq. (2). This implies that the full BE can be converted completely into a Boolean master equation. This conversion is carried out on the microscale of a nearest-neighbor cellular automaton and consists of two steps. First, the deterministic motion of the particles gets replaced by appropriate probabilistic scattering events in such a way that the equations of motion, Eq. (4), are obeyed on the macroscale. In a second step, the lengths and momenta in the kinematic terms Eq. (3) of the BE are rescaled such as to minimize the statistical fluctuations introduced by the first step.

In order to convert the Boltzmann equation (BE) to an automaton, we start by discretizing it with respect to time, position and Bloch momentum. All \mathbf{x} and \mathbf{k} derivatives in Eqs. (1)-(4) are replaced by finite difference vectors $\Delta\mathbf{x} = |\Delta\mathbf{x}|\dot{\mathbf{x}}/|\dot{\mathbf{x}}|$ and $\Delta\mathbf{k} = |\Delta\mathbf{k}|\dot{\mathbf{k}}/|\dot{\mathbf{k}}|$. In addition, we define lattice cells in \mathbf{x} space and \mathbf{k} space with volumes $V_{\mathbf{R}}$ and $V_{\mathbf{K}}$ which are labeled by their cell centers \mathbf{R} and \mathbf{K} , respectively. By integrating f over a phase space cell (\mathbf{R},\mathbf{K}) , one obtains the cell integrated occupancy,

$$N_{\mathbf{R},\mathbf{K}}(t) = \int_{V_{\mathbf{R}}} d\mathbf{x} \int_{V_{\mathbf{K}}} \frac{d\mathbf{k}}{(2\pi)^3} f(\mathbf{x}, \mathbf{k}; t) = \frac{1}{(2\pi)^3} V_{\mathbf{R}} V_{\mathbf{K}} f(\mathbf{R}, \mathbf{K}; t) , \quad (5)$$

where the last equality holds for sufficiently small cells. In terms of $N_{\mathbf{R},\mathbf{K}}$, the cell integrated BE takes the form

$$N_{\mathbf{R},\mathbf{K}}(t + \Delta t) = N_{\mathbf{R},\mathbf{K}}(t) + \Delta N_{\mathbf{R},\mathbf{K}}^D(t) + \Delta N_{\mathbf{R},\mathbf{K}}^E(t) + \Delta N_{\mathbf{R},\mathbf{K}}^C(t) , \quad (6)$$

where the indices D, E and C are the diffusion-induced, field-induced, and collision-induced contributions to the BE, respectively.

The collision term can easily be expressed in terms of $N_{\mathbf{R},\mathbf{K}}$ and the cell-integrated scattering probabilities $P_{\mathbf{K}'\mathbf{K}}$,

$$\Delta N_{\mathbf{R},\mathbf{K}}^C(t) = \sum_{\mathbf{K}'} \{ P_{\mathbf{K}'\mathbf{K}}^C(\mathbf{R}) N_{\mathbf{R},\mathbf{K}'}(t) - P_{\mathbf{K}\mathbf{K}'}^C(\mathbf{R}) N_{\mathbf{R},\mathbf{K}}(t) \} , \quad (7)$$

$$P_{\mathbf{K}'\mathbf{K}}^C(\mathbf{R}) = \frac{V}{V_{\mathbf{K}'} V_{\mathbf{R}}} \int_{V_{\mathbf{R}}} d\mathbf{x} \int_{V_{\mathbf{K}}} d\mathbf{k} \int_{V_{\mathbf{K}'}} \frac{d\mathbf{k}'}{(2\pi)^3} w_{\mathbf{k}'\mathbf{k}}(\mathbf{x}) \Delta t . \quad (8)$$

The crucial point is that, after some algebraic manipulations, the term proportional to the applied electric field in Eq. (6) can be also written as [5]

$$N_{\mathbf{R},\mathbf{K}}^E(t) = \sum_{\mathbf{K}'} \{ P_{\mathbf{K}'\mathbf{K}}^E(\mathbf{R}) N_{\mathbf{R},\mathbf{K}'}(t) - P_{\mathbf{K}\mathbf{K}'}^E(\mathbf{R}) N_{\mathbf{R},\mathbf{K}}(t) \} , \quad (9)$$

which has the same form as Eq. (7). In this equation, the particle acceleration appears as effective scattering probability given by

$$P_{\mathbf{K}'\mathbf{K}}^E(\mathbf{R}) = \frac{e|\mathbf{E}(\mathbf{R})|\Delta t}{\hbar\Delta k} \frac{O_{\mathbf{K}'\mathbf{K}}^{\Delta k}}{V_{\mathbf{K}'}} , \quad (10)$$

where $O_{\mathbf{K}\mathbf{K}'}^{\Delta\mathbf{k}}$ is the geometrical overlap in \mathbf{k} -space of the cell \mathbf{K}' and the cell \mathbf{K} which has been rigidly shifted by an amount $-\Delta\mathbf{k}$ and is now centered at $\mathbf{K}-\Delta\mathbf{k}$. Importantly, this Eq. (10) is scale invariant with respect to the momentum grid spacing Δk . This observation can be utilized to minimize the statistical fluctuations. With an appropriate choice for Δk , one finally obtains [5]

$$P_{\mathbf{K}'\mathbf{K}}^E(\mathbf{R}) = \frac{\Delta t}{\tau_{free}(\mathbf{R}, \mathbf{K}')} \frac{O_{\mathbf{K}'\mathbf{K}}^{\Delta\mathbf{k}}}{V_{\mathbf{K}'}} , \quad (11)$$

where $\tau_{free}(\mathbf{R}, \mathbf{K})$ is the mean time of free flight in the phase space cell (\mathbf{R}, \mathbf{K}) . The Equations (9) and (11) have exactly the form of Eq. (7) and are local in \mathbf{R} -space. In an analogous way, one can rewrite the diffusion related term in the BE as [5]

$$\Delta N_{\mathbf{R}, \mathbf{K}}^D(t) = \sum_{\mathbf{R}'=\mathbf{R}_{nn}} \{P_{\mathbf{R}'\mathbf{R}}^D(\mathbf{K})N_{\mathbf{R}', \mathbf{K}}(t) - P_{\mathbf{R}\mathbf{R}'}^D(\mathbf{K})N_{\mathbf{R}, \mathbf{K}}(t)\} , \quad (12)$$

$$P_{\mathbf{R}\mathbf{R}'}^D(\mathbf{K}) = \frac{v(\mathbf{K})}{c} \delta((\mathbf{R}' - \mathbf{R})/a, \mathbf{K}/|\mathbf{K}|) , \quad (13)$$

where the sum in Eq. (12) runs over the nearest neighbors \mathbf{R}_{nn} of site \mathbf{R} only. Here, $v(\mathbf{K})$ is the particle's velocity and $c = d/\Delta t$ is the maximum particle velocity in the cellular automaton with lattice constant d and time step Δt .

With Eqs. (7), (9), and (12), the BE has been successfully converted into a master equation which fully incorporates the kinematic terms in the Boltzmann equation. The final step consists in discretizing the cell occupancies $N_{\mathbf{R}, \mathbf{K}}(t)$ by defining integer phase-space cell occupancies $n_{\mathbf{R}, \mathbf{K}}(t)$ and Boolean scattering rates $p = \{0, 1\}$ in such a way that the *average* over an ensemble of CA's yields the continuous quantities, e.g. $\langle n_{\mathbf{R}, \mathbf{K}}(t) \rangle_{CA} = N_{\mathbf{R}, \mathbf{K}}(t)$ [5].

For nonhomogeneous problems, the BE needs to be solved self-consistently with the Poisson equation which gives the electric field $\mathbf{E}(\mathbf{R})$ on the macro-scale of the CA.

C. Results: Comparison with Monte Carlo simulations

We now turn to some tests and applications of the CA method for n-type GaAs. We have carried out both CA simulations and ensemble Monte Carlo calculations (MC) employing exactly the same materials' parameters [8]. These examples primarily serve the purpose to demonstrate that the CA method is a robust scheme which does not depend critically on the chosen discretization on the micro-scale of the lattice and easily reaches the accuracy of the standard ensemble Monte Carlo technique. In fact, we have purposely chosen a rather crude discretization here.

We took a two-dimensional hexagonal \mathbf{x} -lattice with typically 300×100 lattice sites and a three-dimensional \mathbf{k} -lattice. The 3-D \mathbf{k} -space attached to each lattice site has been divided into 60-degree sectors (corresponding to the 6 neighbors in \mathbf{x} -space) made up of onion-like shells. Each shell represents an energy interval of typically one optical phonon energy (except the first few shells that have a finer energy resolution). Altogether, between 20 and 30 shells have been included for each valley. We have used a non-parabolic three-valley model for the carrier dispersion and included acoustic and optical phonon scattering, as well as ionized impurity scattering. Averages over blocks of 8×8 cells are sufficient in most cases to determine the physical quantities such as velocities, particle densities, or fields on the macro-scale of the CA. The time step was chosen to be two femtoseconds both for the CA or Monte Carlo transport equations as well as for the Poisson equation. The MC simulations were carried out with an ensemble of 10000 particles, whereas typically 100000 were used in the CA simulations.

Due to the limited number of initial and final scattering states in the CA, the total scattering probabilities $P^D + P^F + P^C$ could be stored completely in look-up tables, reducing the simulation to a sheer mapping of Boolean arrays onto one another. The resulting CA-method is very efficient numerically: We found speed-up's of 3.9 in computer time when the program was able to access concurrently 4 processors instead of 1 processor on a Cray-YMP computer.

In Fig. 1, the drift velocity in homogenous n-type GaAs is depicted as a function of the electric field. Overall, the CA simulations can be seen to be in very good agreement with the MC. Compared to MC, the CA results slightly overestimate the low field mobility but underestimate the maximum velocity near 4 kV/cm. Both deviations are a consequence of the coarse graining of the energy space. Since the micro-scale of the CA has an energy resolution of typically one optical phonon energy, the carriers cannot completely thermalize for low fields and do not gain quite as much energy as in MC for high fields.

In Fig. 2, we show the field dependent population of the three valleys in the conduction bands of GaAs. Again, the agreement between the CA and MC simulations is excellent in the whole regime of fields.

These homogeneous transport data do not test the capability of the CA to yield a correct description of transient or diffusive inhomogeneous transport phenomena. Therefore, we show the distribution of carriers in the three conduction band valleys as a function of time in Fig. 3. Starting with a stationary carrier distribution without an applied field, a homogenous electric field of 10 kV/cm is suddenly switched on at time zero. As a result, about 60% of the carriers get scattered from the Γ -valley into the L-valley. Again, MC and CA calculations are in excellent agreement with one another.

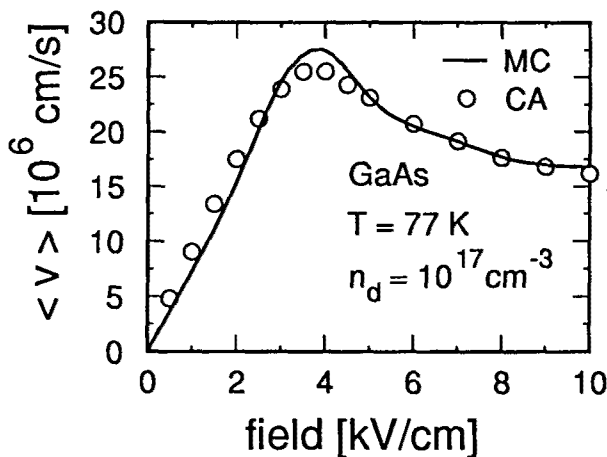


Fig. 1. Calculated drift velocity versus electric field for bulk GaAs at 77 K with a doping density of 10^{17} cm^{-3} . Full lines: Monte Carlo. Circles: cellular automaton simulations.

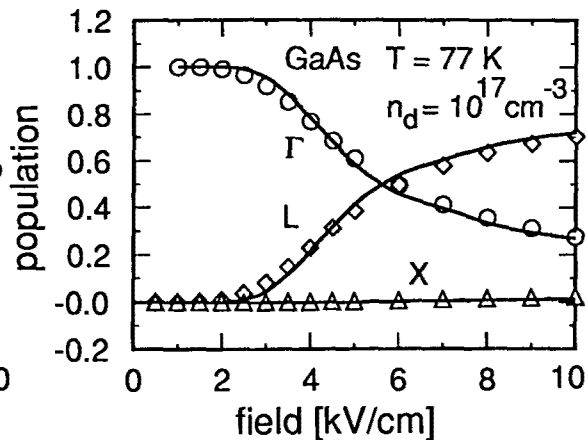


Fig. 2. Calculated carrier population of the Γ , L, and X valleys versus electric field for bulk GaAs with same parameters as in Fig. 1. Full lines: Monte Carlo. Circles, diamonds, triangles: cellular automaton simulations.

Finally, we turn to a simple GaAs device in order to test the overshoot behaviour in CA simulations for inhomogeneous transport. In Fig. 4, we show the drift velocity versus position for a 0.25/0.40/0.25 μm n-i-n structure. The voltage drop is 0.5 V across this device. The doping concentrations are $1 \times 10^{17} \text{ cm}^{-3}$ in the n-regions and $1 \times 10^{15} \text{ cm}^{-3}$ in the i-zones, respectively. In the CA simulation, we chose 180 cells in x-space along the n-i-n structure and only 6 cells perpendicular to it since the inhomogeneity is one-dimensional. Both MC and CA simulations show that the electric field varies between 10 kV/cm and -25 kV/cm in the intrinsic zone. This leads to a strong velocity overshoot which is predicted by

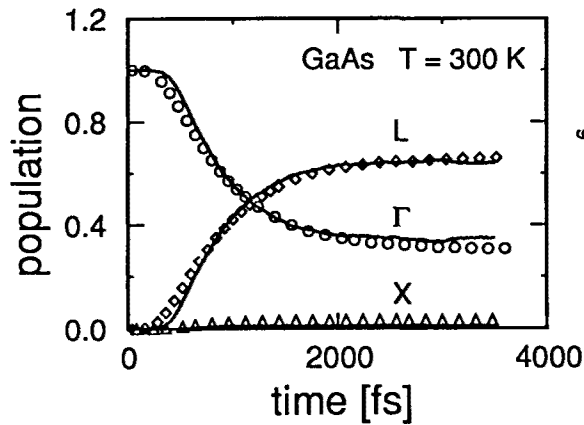


Fig. 3. Calculated transient carrier population of the Γ , L, and X valleys in GaAs at $T=300$ K for a suddenly switched on electric field of 10 kV/cm. Full lines: Monte Carlo. Circles, diamonds, triangles: Cellular automaton simulations.

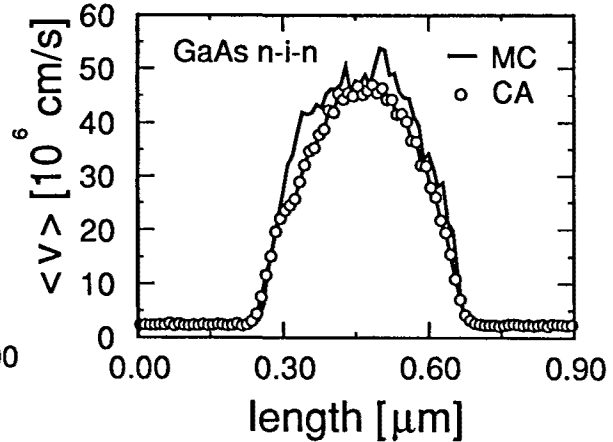


Fig. 4. Drift velocity as a function of position in a $0.9 \mu\text{m}$ GaAs n-i-n structure at $T=77$ K. The applied voltage is 0.5 V, and the n-doping density is $n_d=1 \times 10^{17} \text{ cm}^{-3}$.

both methods. Similar to our earlier finding (Fig. 1), the presently chosen energy discretization in the CA leads to a slightly lower velocity than obtained by the Monte Carlo method.

In conclusion, we have presented a novel simulation technique for semiclassical transport based on cellular automata. This method is tailored to a quantitative assessment of highly nonlinear stationary as well as transient transport phenomena including the dynamics of domains in semiconductors.

We are indebted to Prof. Paolo Lugli for his valuable help and critical discussions. This work was supported by the Deutsche Forschungsgemeinschaft, Project Vo 483/1-1.

References

- ¹ U. Frisch, B. Hasslacher, and Y. Pomeau, Phys. Rev. Lett. **56**, 1505 (1986).
- ² U. Frisch, D. d'Humières, B. Hasslacher, P. Lallemand, Y. Pomeau, and J.P. Rivet, Complex Systems **1**, 649 (1987).
- ³ J. Hardy, O. de Pazzis, and Y. Pomeau, Phys. Rev. **A13**, 1949 (1976).
- ⁴ For recent reviews, see *Lattice Gas Methods for PDE's: Theory, Application, and Hardware*, edited by G. D. Doolen, Physica D **45** (1990).
- ⁵ K. Kometer, G. Zandler, and P. Vogl, Phys. Rev. **B 46**, issue July 15, (1992), in print.
- ⁶ C. Jacoboni and L. Reggiani, Rev. Mod. Phys. **55**, 645 (1986).
- ⁷ C. Jacoboni and P. Lugli, *The Monte Carlo Method for Semiconductor Device Simulation* (Springer, 1989, Vienna).
- ⁸ M. A. Littlejohn, J. Hauser, and T. H. Glisson, J. Appl. Phys. **48**, 4587 (1977).